IEEE Access
Multidisciplinary | Rapid Review | Open Access Journal

Received March 29, 2022, accepted April 9, 2022, date of publication April 13, 2022, date of current version April 20, 2022.

Digital Object Identifier 10.1109/ACCESS.2022.3167170

Automatic Segmentation of Nonstationary EM Emission of Electronics Product

TITO YUWONO[1,2], MOHD HAFIZ BAHARUDDIN[1], NORBAHIAH MISRAN[1], (Senior Member, IEEE), MAHAMOD ISMAIL[1], (Senior Member, IEEE), DAVID W. P. THOMAS[3], (Senior Member, IEEE), CHRISTOPHER SMARTT[3], AND HRISTO ZHIVOMIROV[4], (Member, IEEE)

[1]Department of Electrical, Electronic, and System Engineering, Faculty of Engineering and Built Environment, Universiti Kebangsaan Malaysia, Bangi 43600, Malaysia
[2]Department of Electrical Engineering, Islamic University of Indonesia, Yogyakarta 55584, Indonesia
[3]George Green Institute for Electromagnetics Research, University of Nottingham, Nottingham NG7 2RD, U.K.
[4]Department of Theory of Electrical Engineering and Measurements, Technical University of Varna, 9010 Levski, Bulgaria

Corresponding author: Mohd Hafiz Baharuddin (hafizb@ukm.edu.my)

This work was supported in part by the Geran Universiti Penyelidikan Universiti Kebangsaan Malaysia (UKM) under Grant GUP-2019-021, and in part by the Geran Galakan Penyelidik Muda Universiti Kebangsaan Malaysia (UKM) under Grant GGPM-2020-005.

ABSTRACT Characterizing complex and multi-functional devices is a very challenging task. One problem in statistical near field analysis on complex electronic products is the emergence of nonstationary electromagnetic (EM) signals. Such emergence will lead to an incorrect decision if the signal is used as an input to propagation analysis. The most appropriate approach to this problem seems to be one based on the segmentation of the nonstationary time series obtained from measurements into an ensemble of piecewise stationary signals. In this paper, we propose three approaches for automatic segmentation of nonstationary EM emission signals: short-time energy (STE), short-time zero-crossing rate (STZCR), and short-time kurtosis (STK). Test results show that STE is the best in terms of success in segmenting the nonstationary signals to achieve piecewise stationary time series and being less computationally intensive.

INDEX TERMS Automatic segmentation, nonstationary, EM emission, electronic product.

I. INTRODUCTION

The use of modern and complex electronic products is widespread. In particular, with the presence of the Internet of Thing (IoT) system, products have many telecommunication technology platforms, such as bluetooth, wireless fidelity (WiFi), long range (LoRa), and cellular components. Managing complex electronic products that must meet electromagnetic compatibility (EMC) requirements is challenging for EMC engineers. They need to ensure that the emissions of an electronic product do not exceed EMC requirements to avoid interference to the product itself and the products around it. In addition, the product must work well in its electromagnetic (EM) radiation environment.

Several techniques are available for measuring EM emissions, namely, open area test site (OATS), anechoic chamber (AC), compact antenna test range (CATR), transverse electromagnetic (TEM) cells, reverberation chamber (RC), and near-field scanning (NFS). Each method has its characteristics, advantages, disadvantages, and suitability to the Device Under Test (DUT).

Several studies and applications of OATS can be found in [1]–[6]. Techniques and analysis using AC can be found in [7]–[13]. The study and application of CATR can be found in [14]–[21]. The study and application of TEM cells can be found in [22]–[30]. The study and application of RC can be found in [31]–[37]. The study and application of the NFS technique can be found [38]–[51].

Based on the size of the test area, OATS has the largest area, while TEM cell, CATR, and NFS have the narrowest area. Based on installation costs, OATS and AC have relatively high installation costs, whereas TEM cell, CATR, and NFS have low installation costs.

NFS is one of the recommended measurement techniques for EM emissions during the development of electronic products. The advantages of using this technique are that

The associate editor coordinating the review of this manuscript and approving it for publication was Wen-Sheng Zhao.

it is more economical and can be used to locate emission sources from electronic assemblies. These advantages cannot be achieved by using other far-field measurement techniques such as OATS or AC. Data from NFS can be used to characterise complex and multi-functional devices. A statistical description of EM sources may be used to analyze random sources. An algorithm for propagating the statistical properties of EM fields based on Wigner Functions has been described in [52], and [53]. This algorithm is used to propagate field–field correlation functions from the NFS measurement plane. The field–field correlation function can be provided through measurement by one- [54] and two-probe measurements [40], [55]. However, providing the field–field correlation function as input for the propagation algorithm requires the emission process to be stationary, which is very often not the case in real-world systems. One way to achieve stationary emissions is by controlling the mode of operation of the device. However, this situation is not always the case for real-life applications because the device can be multi-functional and has different modes of operation at different times. A previous study has discussed [56] that using a nonstationary series as an input for the method designed for stationary series can lead to misleading results. For example, a process with high emissions may only occur for a small percentage of the time. However, the average process in calculating the field–field correlation would reduce the influence of this process under the assumption of stationary emissions statistics.

An approach based on the segmentation of the nonstationary time series obtained from measurements into an ensemble of piecewise stationary time series seems to be an appropriate viable approach to dealing with this issue. That is, a piecewise stationary mode is used for the emissions of the device. Some techniques on the analysis of nonstationary time series discussed in [57] and [58] have been previously implemented in speech processing and for detecting the arrival phases in earthquakes, respectively. In [57]–[59], a segmentation algorithm can be applied to the nonstationary time series to achieve the piecewise-stationary time series.

Figure 1 shows the phenomenon of nonstationary emissions resulting from the operating of a Galileo microcontroller [60]. In the present study, a segmentation technique to achieve piecewise stationary from the nonstationary emissions was carried out manually where signals in the time domain are divided into 16 segments. Manual segmentation for detection of nonstationary signals is shown in Figure 2. This method is able to sort short time segments based on their stationary characteristics. However, segmenting the data uniformly can cause some of the high emissions signals to be divided into two parts. Dividing the data so that the chosen change points essentially match its actual locations is the ideal approach. Therefore, further improvement to the segmentation procedure is needed to determine the change points in the nonstationary time-domain data automatically rather than simply sorting the manually grouped subsets of data.

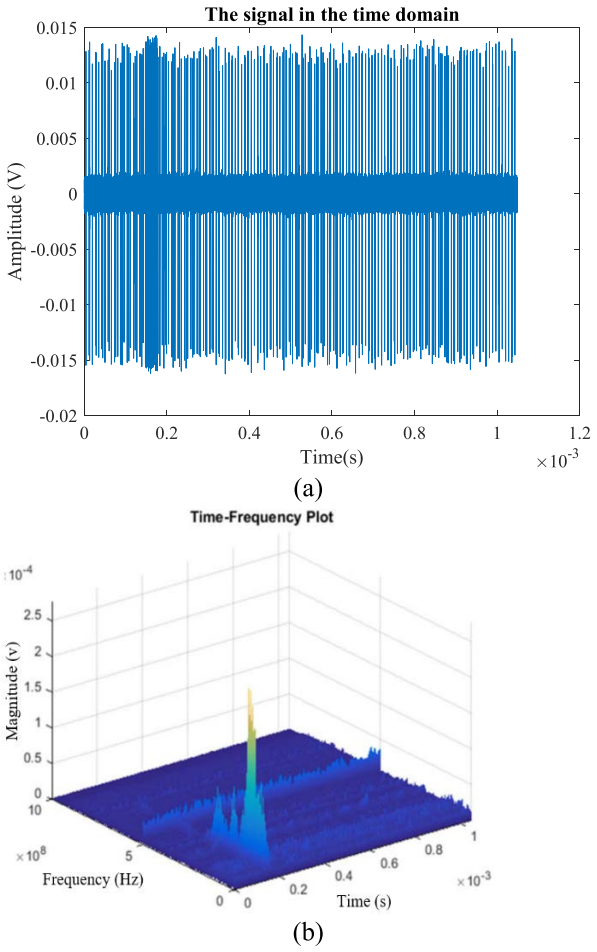

FIGURE 1. Nonstationary emissions from Intel Galileo: a) Time domain b) Time-frequency domain [60].

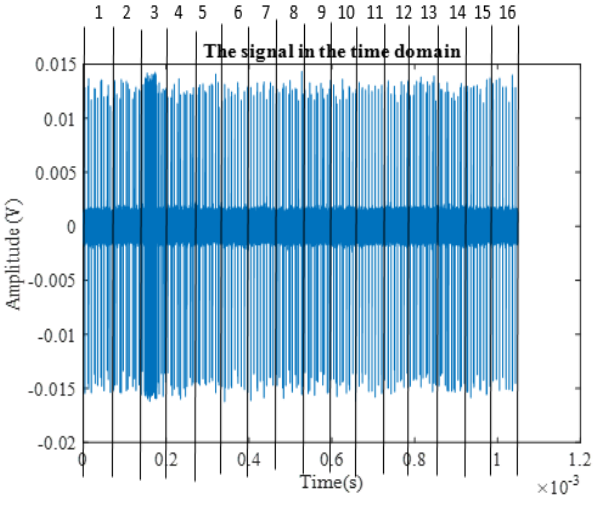

FIGURE 2. Signal time series from measurement divided by 16 segments manually [60].

In this work, the main focus is to obtain a piecewise stationary model of emissions by implementing automatic

segmentation techniques. Three different types of segmentation techniques were introduced. They are based on STE, STZCR and STK.

This paper is divided into four sections. The first section introduces emissions measurement. The second section is the methodology. The third section is the results and discussion. The last section is the conclusion.

II. STE, STZCR, AND STK

We extract signal frames (segments) at regular intervals using a time-limited window function $w[m]$, expressed as [61]:

$$x_f[m] = w[m]\, x[m + fh] \tag{1}$$

where $m \in \{1, \ldots, M\}$ is the local time index (i.e., an index relative to the start of the sliding extraction window), M is the window length, f is the frame index, and h is the hop size (i.e., the time advance, expressed in samples, from one signal frame to the next).

STE is defined as the energy of the corresponding signal frame [62]:

$$STE[f] = \sum_m x_f[m]^2 \tag{2}$$

STE is commonly used to classify speech signals [62]–[66]. Figure 3 shows the waveform of author speech of the word "Hello I am Tito" and its STE. The use of STE for vibration analysis can be found in [67]. STE is also used for high-frequency detection for intracranial electroencephalography [68].

STZCR is another technique that can measure the noisiness of a signal in the time domain. STZCR is defined as the number of times the zero axis is crossed per frame [69]. STZCR is a very simple measure of the fundamental frequency of the signal. In the context of discrete signal time, zero crossing occurs when the previous sample has a different algebraic sign from the current sample. For example, if x is a sample signal, then zero crossing occurs when x[i] is a positive number and x[i-1] is negative and vice versa [70]. Figures 4 and 5 show the concept of the zero crossing and zero crossing rate (ZCR).

Mathematically, STZCR is defined as the ZCR of the signal frame under consideration [71]:

$$STZCR[f] = \sum_m |sgn(x[m]) - sgn(x[m-1])| \tag{3}$$

where sgn(•) is the signum function.

Like STE, STZCR is widely used for speech analysis. Several studies related to the use of STZCR can be found in [62], [72]–[75].

STK is also considered in this paper. The concept of kurtosis was discovered by Karl Pearson and Walter F. R. Weldon [76]. Kurtosis is defined as the ratio of the fourth moment 4 to the square of the variance 4 on the probability distribution of the random variable x. Kurtosis

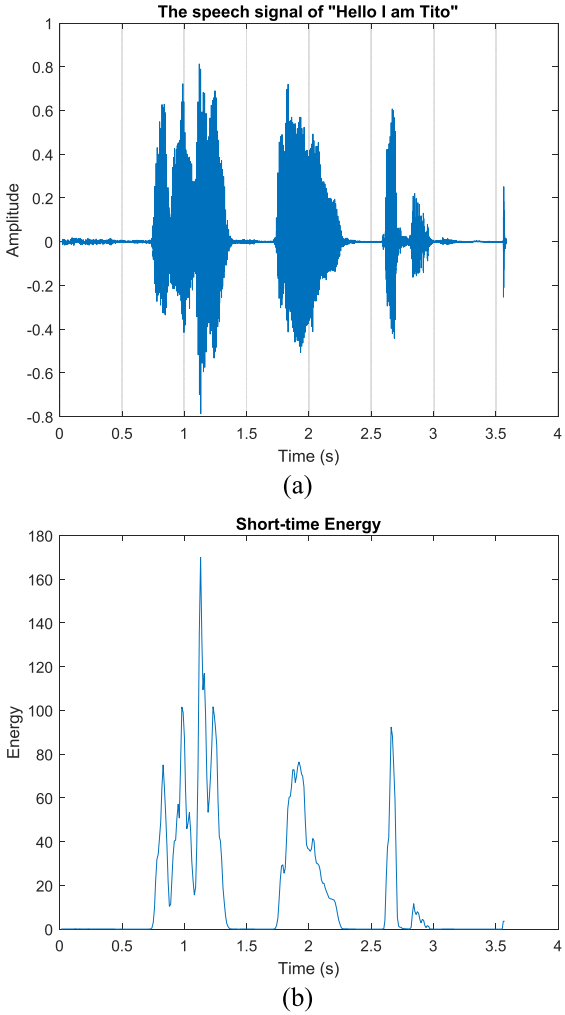

FIGURE 3. (a) Waveform of the uttered word "Hello I am Tito" and (b) STE of speech signal.

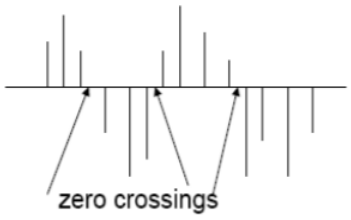

FIGURE 4. Concept of Zero Crossing [70].

can be used as an indicator to show the degree of curvature (*sui generis* peakedness). The greater the kurtosis value, the sharper the curve. The kurtosis is calculated using the ratio of the fourth-order moment to the square of the second-order moment [77].

Mathematically, the STK is defined as the kurtosis of the signal frame of interest [77], [78]:

$$STK[f] = \frac{\sum_m (x_f[m] - m_{x_f})^4 / M}{S_{x_f}^4} \tag{4}$$

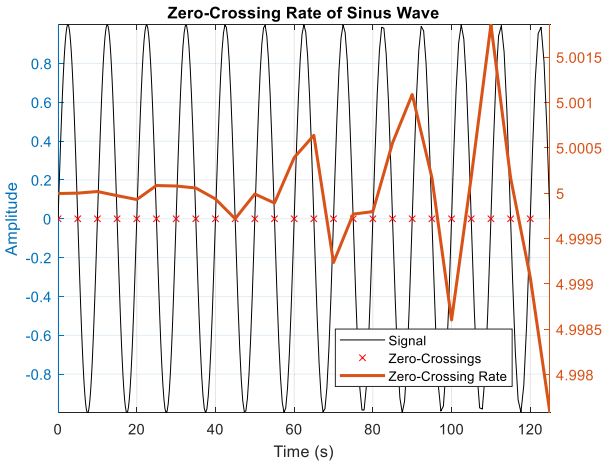

FIGURE 5. Concept of STZCR.

where:

m_{x_f} is the sample mean of the corresponding signal frame;

s_{x_f} is the standard deviation of the corresponding signal frame.

The reference value of kurtosis is 3. If the value of kurtosis is greater than 3, then the distribution curve is called leptokurtosis. If it is lower than 3, it is called platy kurtosis. The kurtosis value is equal to 3 curves indicating a normal or meso kurtosis distribution curve. Figure 6 shows the concept of kurtosis.

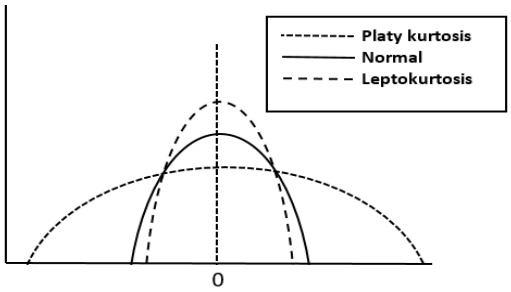

FIGURE 6. Concept of kurtosis.

III. RESEARCH METHOD

In this paper, multiple nonstationary EM emissions signals were tested. They were measured from Intel Galileo and Raspberry Pi microcontroller boards using an oscilloscope and a magnetic field probe. The probe to measure the EM emissions, which is connected to channel 1 of an 8 GHz KEYSIGHT DSOS804a Digital Oscilloscope, is a Langer EMV-Technic RF R50-1 magnetic field probe. A task or program that can produce nonstationary EM emissions is uploaded to the board so that the sorting technique can be implemented. EM emission data from measurement are stored in oscilloscope memory in.bin format. This data will later be segmented to sort each nonstationary signal into two or more piecewise stationary subsets. Figures 7 and 8 show both boards and the positioning of the probe during the measurement process. The flow of the automatic segmentation algorithm is shown in Figure 9.

FIGURE 7. Intel galileo board.

FIGURE 8. Raspberry Pi 3 board.

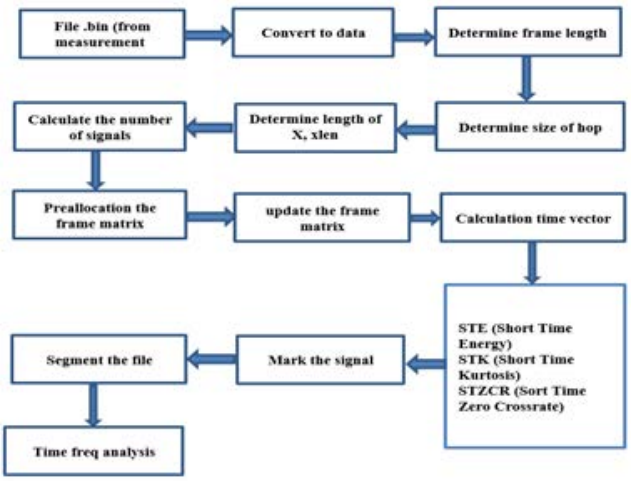

FIGURE 9. Flow of automatic segmentation algorithm.

We have taken four samples of nonstationary EM signals with different characters to test the performance of the

automatic segmentation. Figures 10–13 show four samples of nonstationary EM signals that were obtained from measurements. All four samples seem to have short duration emissions characterized by an increased density in the time domain data plots that occur at a random time. From the time domain data, the signal of interest is present at the end, beginning, beginning and end, and at the end of the data, as shown in Figures 16–19.

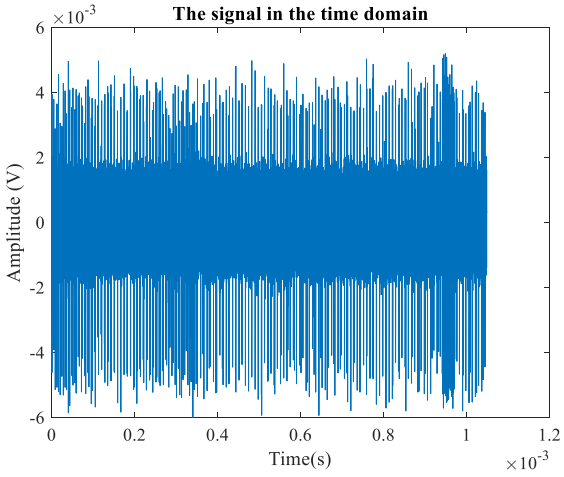

FIGURE 10. Nonstationary signal with position of signal of interest at right (from galileo) (Case 1).

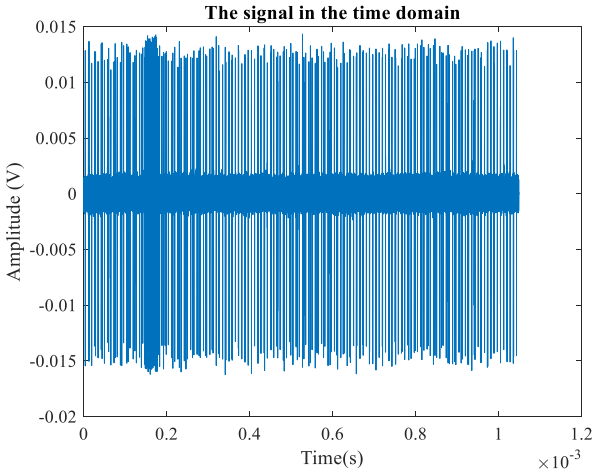

FIGURE 11. Nonstationary signal with position of signal of interest at left (from galileo) (Case 2).

These studies have been carried out using a HP Laptop with an Intel(R) Core(TM) i7 processor and 8 GB RAM. The operating system Windows 10 Home was used to run Matlab R2021b. Table 1 shows the parameters of this study.

IV. RESULTS AND DISCUSSIONS

In the previous section, we discussed the development of algorithms for detection of nonstationary signals with automatic segmentation. In this section, we will discuss the performance of the automatic segmentation algorithm using the proposed techniques. The performance includes the ability to do segmentations efficiently and in terms of time needed to complete the task.

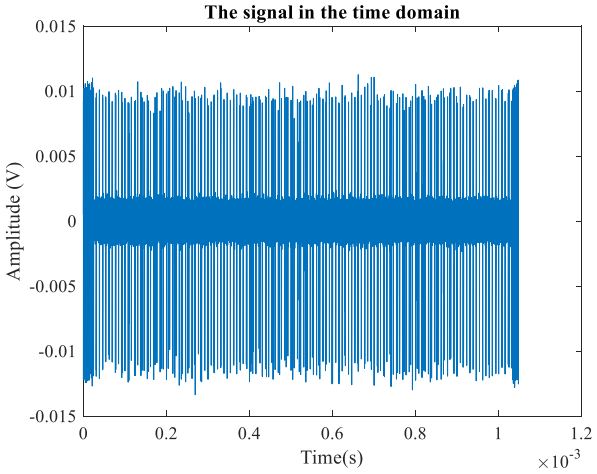

FIGURE 12. Nonstationary signal with position of signal of interest at right and left (from galileo) (Case 3).

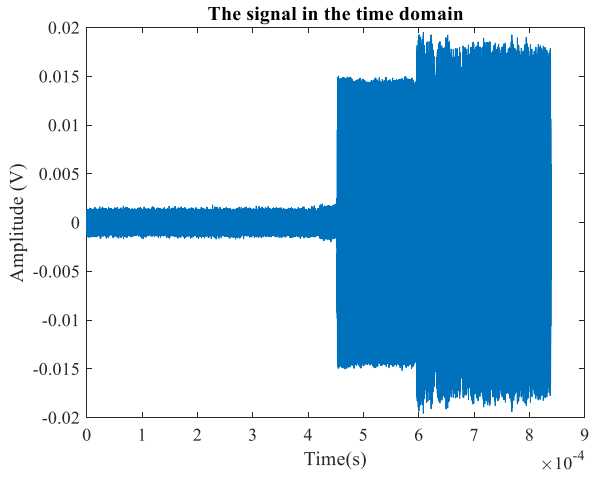

FIGURE 13. Nonstationary signal with position of signal of interest being a wide signal at right (from raspberry Pi) (Case 4).

TABLE 1. Parameters of automatic segmentation algorithm.

Parameters	Value
Number of samples of Case 1, Case 2, Case 3	2^21
Number of samples of Case 4	2^23
Sampling frequency of Case 1, Case 2, and Case 3	2 x 10^9 Hz
Sampling frequency of Case 4	10^{10} Hz
Hop size	20000
Frame length	100000

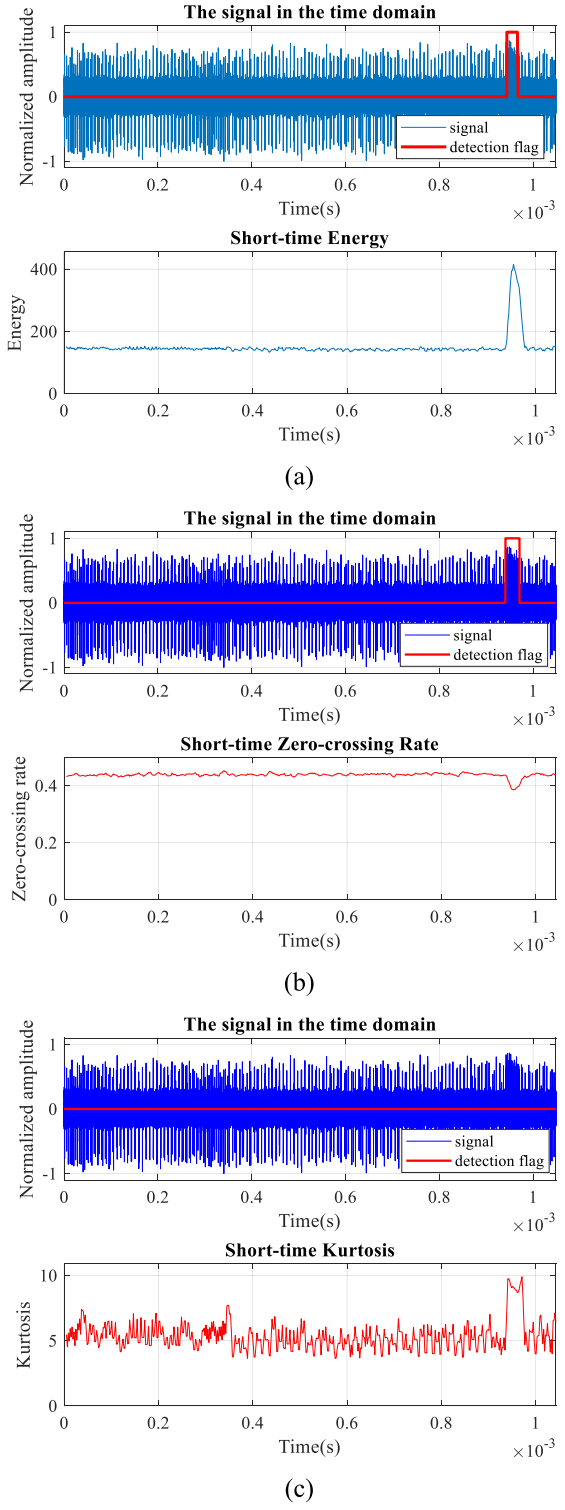

FIGURE 14. Results of automatic segmentation for case I using (a) STE (b) STZR (c) STK.

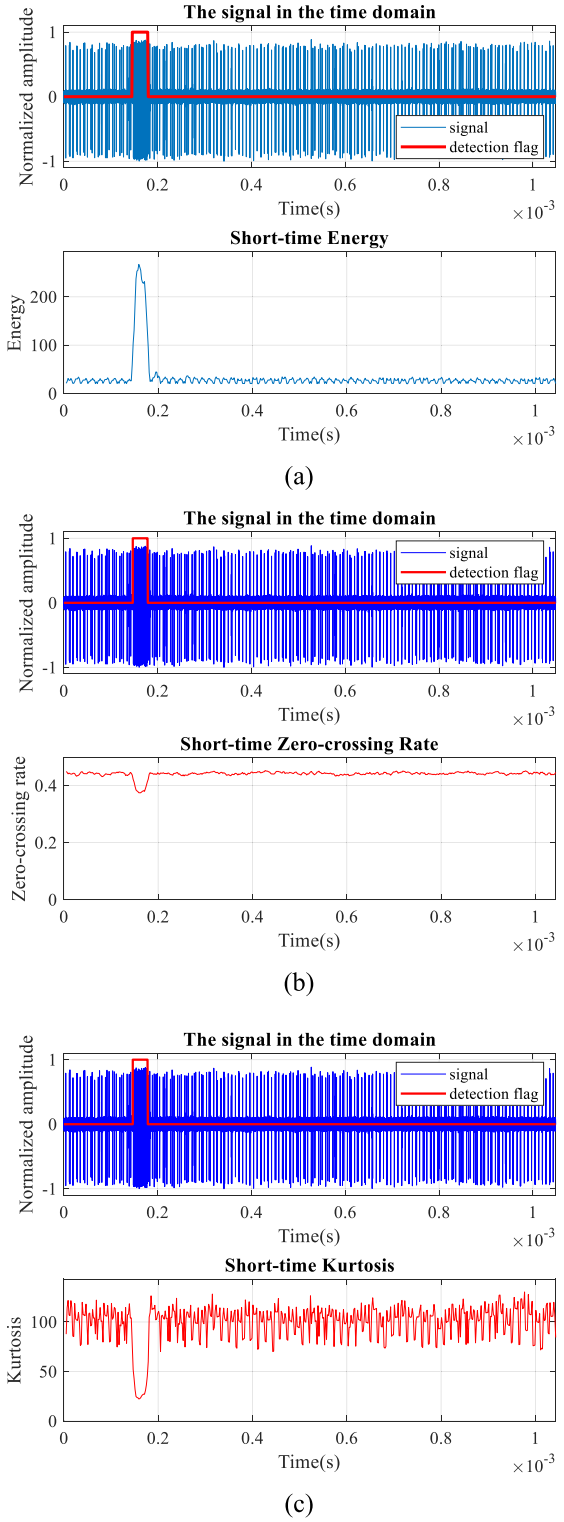

FIGURE 15. Results of automatic segmentation for case II using (a) STE (b) STZR (c) STK.

As described in Section III, the scenario of testing was using four samples of nonstationary signals with different characteristics. The first nonstationary signal has a narrow and short duration of emission of interest that is located at the end of the data. The second signal has one at the beginning, and the third signal has one at the beginning and end of the data. The last signal has wide emissions of interest at the end of the data.

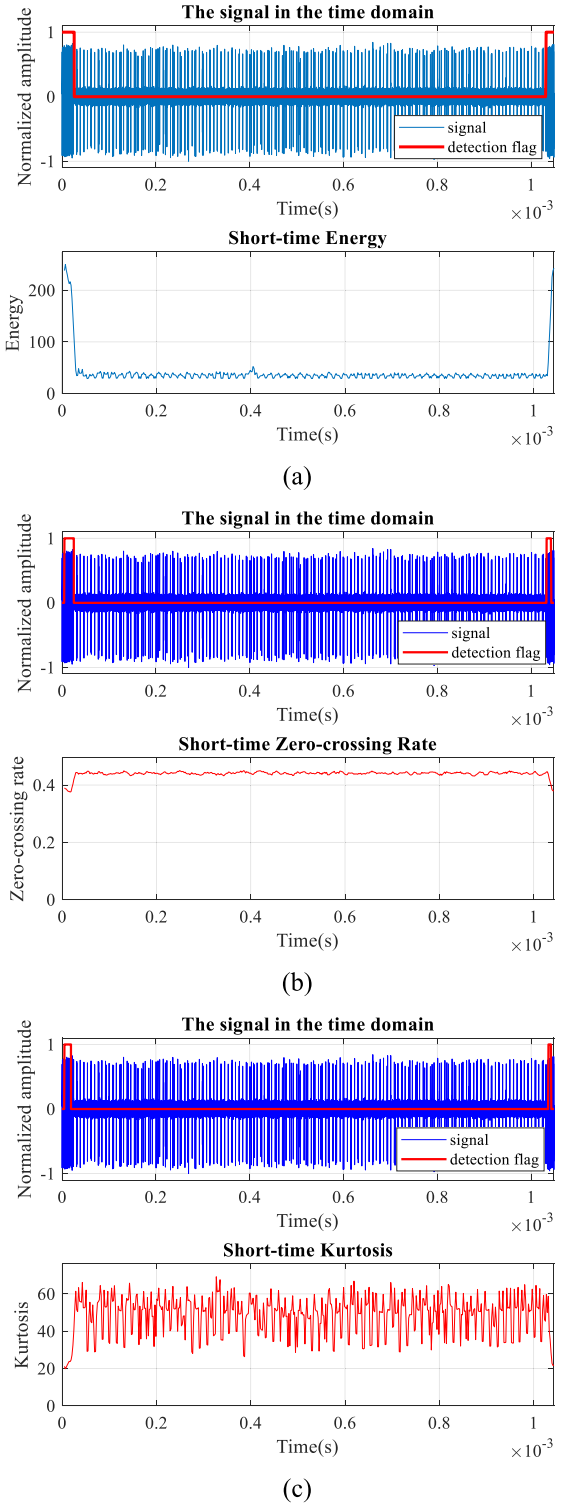

FIGURE 16. Results of automatic segmentation for case III using (a) STE (b) STZR (c) STK.

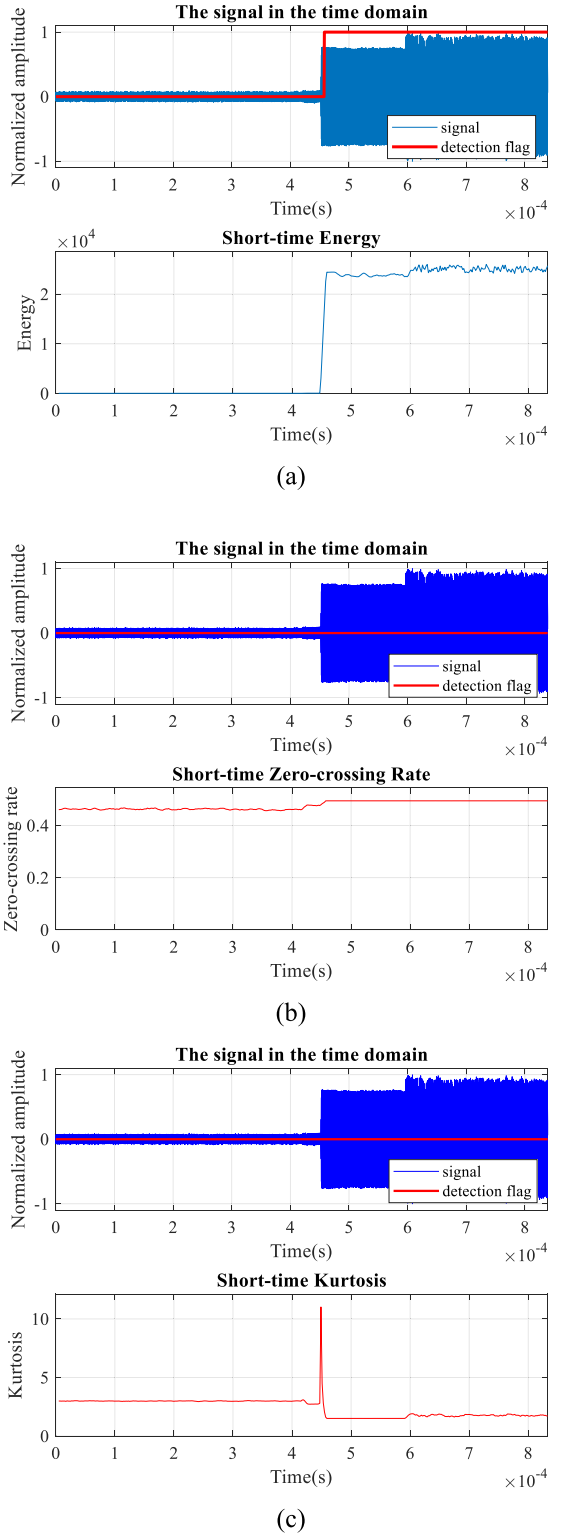

FIGURE 17. Results of automatic segmentation for case IV using (a) STE (b) STZR (c) STK.

A. AUTOMATIC SEGMENTATION FOR NONSTATIONARY SIGNAL WITH POSITION OF SIGNAL OF INTEREST AT RIGHT POSITION

In the first case, the nonstationary signal is narrow and positioned at the end of the time domain signal. The result of the automatic segmentation is shown in Figure 14. STE and STZCR have successfully segmented the signal of interest and divided the whole signal into two activities. However,

STK failed to segment the signal. The time needed for the implementation of STE, STZCR, and STK is 0.457 s, 0.443 s, and 0.812 s, respectively.

B. AUTOMATIC SEGMENTATION FOR NONSTATIONARY SIGNAL WITH POSITION OF SIGNAL OF INTEREST AT LEFT POSITION

For the second case, the short duration signal of interest is also narrow and positioned at the beginning. The results of automatic segmentation are shown in Figure 15. STE, STZCR, and STK have successfully segmented the whole signal into two regions. The time needed to complete the segmentation process using STE, STZCR, and STK is 0.412 s, 0.423 s, and 0.834 s, respectively.

C. AUTOMATIC SEGMENTATION FOR NONSTATIONARY SIGNAL WITH POSITION OF SIGNAL OF INTEREST AT LEFT AND RIGHT POSITION

For the third case, the nonstationary signal is narrow at the beginning and end. The process of segmentation is shown in Figure 16. STE, STZCR, and STK have successfully segmented the whole signal into two different activities. The time to complete the process using STE, STZCR, and STK is 0.455 s, 0.442 s, and 0.830 s, respectively.

D. AUTOMATIC SEGMENTATION FOR NONSTATIONARY SIGNAL WITH WIDE SIGNAL AT RIGHT POSITION

The last case uses the data obtained from the Raspberry Pi. The signal of interest is a wide signal at the end of the whole signal Figure 17 shows the segmentation process using the three proposed techniques. STE has successfully segmented the whole signal into two activities, whereas STZCR and STK failed to segment the signal. The time needed to complete this process using STE, STZCR, and STK is 1.764 s, 1.378 s, and 2.978 s, respectively.

TABLE 2. Performance of automatic segmentation.

Case	Success (S)/Fail (F)			Running time (s)		
	STE	STZCR	STK	STE	STZCR	STK
Case 1	S	S	F	0.457	0.443	0.812
Case 2	S	S	S	0.412	0.423	0.834
Case 3	S	S	S	0.455	0.442	0.830
Case 4	S	F	F	1.764	1.378	2.978

Table 2 summarizes the performance of automatic segmentation using STE, STZCR, and STK. All three techniques are compared in terms of their capability to successfully segment the test signal and the time needed to complete the process. Table 1 shows that STE has successfully performed the segmentation in all four cases. STZCR was successful in segmenting the first three cases but failed to do so for case number four. The implementation of STK was successful for Cases 2 and 3. However, it fails to segment the signals in Cases 1 and 4. From the results, we can see that the STE has produced a significant improvement towards the automatic segmentation as compared to STZCR, STK and the manual technique that has been used in [60]. Based on its performance, the STE technique is suitable to be used as a solution to automatic segmentation for the EM emission from an electronic product.

V. CONCLUSION

An automatic segmentation algorithm of nonstationary signals has been tested for four cases. The approach of this algorithm is to use STE, STZCR, and STK. The results of the segmentation show that STE is the best approach in terms of segmentation success and the speed of the segmentation process. Therefore, the STE is suitable for use as part of piecewise-stationary emission analysis for real-world complex electronic products. The next step for this research is to integrate the segmentation algorithm into the EM emission analysis algorithm.

REFERENCES

[1] I. Barbary, L.-O. Fichte, M. Stiemer, S. Lange, M. Schaarschmidt, R. Pape, T. Kleine-Ostmann, and T. Schrader, "On the quality of a real open area test site," in *Proc. IEEE Int. Symp. Electromagn. Compat. (EMC)*, Aug. 2015, pp. 1201–1206, doi: 10.1109/ISEMC.2015.7256340.

[2] F. G. Awan and A. Kiran, "Cancellation of interference for emission measurement in open area test site," *Measurement*, vol. 111, pp. 183–196, Dec. 2017, doi: 10.1016/j.measurement.2017.07.037.

[3] D. Meng, X. Liu, and D. Li, "Research on unwanted reflections in an OATS for precise omni antenna measurement," in *Proc. IEEE 6th Int. Symp. Microw., Antenna, Propag., EMC Technol. (MAPE)*, Oct. 2015, pp. 245–249, doi: 10.1109/MAPE.2015.7510308.

[4] I. A. Wibowo, M. Z. M. Jenu, A. Kazemipour, and A. F. A. Rahim, "The application of wire mesh ground plane in open area test site for radiated emission measurement," in *Proc. IEEE Int. RF Microw. Conf.*, Dec. 2011, pp. 13–18, doi: 10.1109/RFM.2011.6168684.

[5] P. Wilson, "On correlating TEM cell and OATS emission measurements," *IEEE Trans. Electromagn. Compat.*, vol. 37, no. 1, pp. 1–16, Feb. 1995, doi: 10.1109/15.350235.

[6] *ANSI, American National Standard for Electromagnetic Compatibility—Open-Area Test site Measurements—Guide for the Computation of Errors American National Standard Guide for the Computation of Errors in Open—Area Test Site Measurements*, Inst. Elect. Electron. Eng., New York, NY, USA, 1988.

[7] K. Malaric, D. Muha, B. Saravanja, and T. Pusic, "Shielded fabric mini anechoic test chamber," in *Proc. Int. Symp. (ELMAR)*, Sep. 2019, pp. 81–84, doi: 10.1109/ELMAR.2019.8918649.

[8] S. Arsalane, N. Arsalane, M. Rifi, and H. Bouassam, "Implementation of a simulated model for the evaluation of electromagnetic disturbances in anechoic chamber," in *Proc. Int. Conf. Syst. Collaboration Big Data, Internet Things Secur. (SysCoBIoTS)*, Dec. 2019, pp. 1–6, doi: 10.1109/SysCoBIoTS48768.2019.9028030.

[9] G. Kumar B., "Challenges in interlab comparison of radiated emission measurement above 1GHz," in *Proc. 13th Int. Conf. Electromagn. Interference Compat. (INCEMIC)*, Jul. 2015, pp. 150–155, doi: 10.1109/INCEMIC.2015.8055868.

[10] L. H. Hemming, *Electromagnetic Anechoic Chambers*. Piscataway, NJ, USA: IEEE Press, 2010.

[11] C. Viswanadham and M. Rao, "Design, simulation and experimental results of UWB rectangular anechoic chamber," *IEEE Electromagn. Compat. Mag.*, vol. 4, no. 3, pp. 41–51, Nov. 2015, doi: 10.1109/MEMC.2015.7336755.

[12] A.-M. Silaghi, C. Balan, E. Tolan, and A. De Sabata, "The influence of measurement setups in radiated emissions testing," in *Proc. 14th Int. Conf. Eng. Modern Electric Syst. (EMES)*, Jun. 2017, pp. 220–223, doi: 10.1109/EMES.2017.7980419.

[13] Z. Xiong, J. Chen, and Z. Chen, "Low frequency modeling for electromagnetic analysis of arbitrary anechoic chambers," in *Proc. IEEE Int. Symp. Electromagn. Compat. (EMC)*, Jul. 2016, pp. 13–18, doi: 10.1109/ISEMC.2016.7571567.

[14] T. M. Gemmer and D. Heberling, "Accurate and efficient computation of antenna measurements via spherical wave expansion," *IEEE Trans. Antennas Propag.*, vol. 68, no. 12, pp. 8266–8269, Dec. 2020, doi: 10.1109/TAP.2020.2996914.
[15] A. F. Vaquero, M. Arrebola, M. R. Pino, R. Florencio, and J. A. Encinar, "Demonstration of a reflectarray with near-field amplitude and phase constraints as compact antenna test range probe for 5G new radio devices," *IEEE Trans. Antennas Propag.*, vol. 69, no. 5, pp. 2715–2726, May 2021, doi: 10.1109/tap.2020.3030969.
[16] C. Rowell, B. Derat, and A. Cardalda-Garcia, "Multiple CATR reflector system for multiple angles of arrival measurements of 5G millimeter wave devices," *IEEE Access*, vol. 8, pp. 211324–211334, 2020, doi: 10.1109/ACCESS.2020.3038597.
[17] S. F. Gregson, C. G. Parini, and S. Pivnenko, "Small antenna testing in a compact antenna test range," in *Proc. Antenna Meas. Techn. Assoc. Symp. (AMTA)*, Oct. 2019, pp. 1–6, doi: 10.23919/AMTAP.2019.8906487.
[18] Y. Hu, S. Wang, and S. An, "Over the air testing and error analysis of 5G active antenna system base station in compact antenna test range," in *Proc. Photon. Electromagnetics Res. Symp.-Fall (PIERS-Fall)*, Dec. 2019, pp. 1007–1010, doi: 10.1109/PIERS-Fall48861.2019.9021378.
[19] J. Zhao and Z. Dong, "Efficient sampling schemes for 3-D ISAR imaging of rotating objects in compact antenna test range," *IEEE Antennas Wireless Propag. Lett.*, vol. 15, pp. 650–653, 2016, doi: 10.1109/LAWP.2015.2466107.
[20] C. Liu and X. Wang, "Design and test of a 0.3 THz compact antenna test range," *Prog. Electromagn. Res. Lett.*, vol. 70, pp. 81–87, 2017, doi: 10.2528/PIERL17080504.
[21] J. Zhao and M. Zhang, "Performance 3-D ISAR imaging in compact antenna test range via compressed sensing," in *Proc. IEEE 17th Int. Conf. Commun. Technol. (ICCT)*, Oct. 2017, pp. 736–740, doi: 10.1109/ICCT.2017.8359735.
[22] M. Koohestani, R. Perdriau, J.-L. Levant, and M. Ramdani, "A novel passive cost-effective technique to improve radiated immunity on PCBs," *IEEE Trans. Electromagn. Compat.*, vol. 61, no. 6, pp. 1733–1739, Dec. 2019, doi: 10.1109/TEMC.2018.2882732.
[23] W. X. Fang, Y. En, Y. Huang, Y. Liu, Y. Chen, P. Lai, H. Qiu, and C. Shi, "Orientation effect of field-to-line coupling in a TEM cell," *IEEE Trans. Electromagn. Compat.*, vol. 59, no. 3, pp. 970–979, Jan. 2017, doi: 10.1109/TEMC.2016.2633062.
[24] A. A. Takach, F. Ndagijimana, J. Jomaah, and M. Al-Husseini, "Position optimization for probe calibration enhancement inside the TEM cell," in *Proc. IEEE Int. Multidisciplinary Conf. Eng. Technol. (IMCET)*, Nov. 2018, pp. 1–5, doi: 10.1109/IMCET.2018.8603026.
[25] M. Koohestani, M. Ramdani, P. Besnier, J.-L. Levant, and R. Perdriau, "Perturbations of electric and magnetic fields due to the presence of materials in TEM cells," *IEEE Trans. Electromagn. Compat.*, vol. 62, no. 4, pp. 997–1006, Aug. 2020, doi: 10.1109/TEMC.2019.2928215.
[26] R. Blecic, H. Stimac, R. Gillon, B. Nauwelaers, and A. Baric, "Improved estimation of radiated fields of unintentional radiators by correction of the impedance mismatch between a transverse electromagnetic cell and a hybrid coupler," *IEEE Trans. Electromagn. Compat.*, vol. 60, no. 6, pp. 1717–1725, Dec. 2018, doi: 10.1109/TEMC.2017.2769021.
[27] Y. Li, J. Wu, H. Li, H. Zhang, H. Ma, and J. Wu, "Comparison test and error analysis of the TEM cell method in IC radiated emission," in *Proc. IEEE Int. Symp. Electromagn. Compat. IEEE Asia–Pacific Symp. Electromagn. Compat. (EMC/APEMC)*, May 2018, pp. 1208–1211, doi: 10.1109/ISEMC.2018.8393980.
[28] M. Stojanovic, F. Lafon, S. O. Land, R. Perdriau, and M. Ramdani, "Determination of equivalent coupling surface of passive components using the TEM cell," *IEEE Trans. Electromagn. Compat.*, vol. 60, no. 2, pp. 298–309, Apr. 2018, doi: 10.1109/TEMC.2017.2714760.
[29] R. Tani, I. Wu, K. Gotoh, Y. Matsumoto, S. Ishigami, R. Suga, and O. Hashimoto, "Characteristic improvement on conducted disturbance measuring apparatus using TEM cells," in *Proc. Int. Symp. Electromagn. Compat. (EMC Europe)*, Sep. 2017, pp. 2–5, doi: 10.1109/EMCEurope.2017.8094790.
[30] S. Wen, J. Zhang, and Y. Lv, "The optimization design of septum in TEM cells for IC EMC measurement," in *Proc. 7th Asia–Pacific Conf. Environ. Electromagn. (CEEM)*, Nov. 2015, pp. 250–253, doi: 10.1109/CEEM.2015.7368677.
[31] A. De Leo, G. Cerri, P. Russo, and V. M. Primiani, "A novel emission test method for multiple monopole source stirred reverberation chambers," *IEEE Trans. Electromagn. Compat.*, vol. 62, no. 5, pp. 2334–2337, Oct. 2020, doi: 10.1109/TEMC.2020.2999651.
[32] L. A. Bronckers, K. A. Remley, B. F. Jamroz, A. Roc'h, and A. B. Smolders, "Uncertainty in reverberation-chamber antenna-efficiency measurements in the presence of a phantom," *IEEE Trans. Antennas Propag.*, vol. 68, no. 6, pp. 4904–4915, Jun. 2020, doi: 10.1109/TAP.2020.2969883.
[33] G. Andrieu, N. Ticaud, F. Lescoat, and L. Trougnou, "Fast and accurate assessment of the 'well stirred condition' of a reverberation chamber from S_{11} measurements," *IEEE Trans. Electromagn. Compat.*, vol. 61, no. 4, pp. 974–982, Jul. 2019, doi: 10.1109/TEMC.2018.2847727.
[34] J. Immidisetti, M. Magdowski, and R. Vick, "Retrofitting a shielded camera enclosure with an internet protocol camera and testing for radiated immunity and emission in a reverberation chamber," *IEEE Int. Symp. Electromagn. Compat.*, Aug. 2018, pp. 849–854, doi: 10.1109/EMCEurope.2018.8485098.
[35] D. Shafei, "The analysis for multimode of electrical fields in reverberating chamber," in *Proc. 4th Int. Conf. Microw. Millim. Wave Technol. (ICMMT)*, Aug. 2018, pp. 74–100, doi: 10.1109/icmmt.2004.1411682.
[36] R. Vogt-Ardatjew, U. Lundgren, S. F. Romero, and F. Leferink, "On-site radiated emissions measurements in semireverberant environments," *IEEE Trans. Electromagn. Compat.*, vol. 59, no. 3, pp. 770–778, Jun. 2017, doi: 10.1109/TEMC.2016.2623380.
[37] D. Senic, D. F. Williams, K. A. Remley, C.-M. Wang, C. L. Holloway, Z. Yang, and K. F. Warnick, "Improved antenna efficiency measurement uncertainty in a reverberation chamber at millimeter-wave frequencies," *IEEE Trans. Antennas Propag.*, vol. 65, no. 8, pp. 4209–4219, Aug. 2017, doi: 10.1109/TAP.2017.2708084.
[38] A. Darvish and A. A. Kishk, "Near-field shielding analysis of single-sided flexible metasurface stopband TE: Comparative approach," *IEEE Trans. Antennas Propag.*, vol. 69, no. 1, pp. 239–253, Jan. 2021, doi: 10.1109/TAP.2020.3000530.
[39] S. Marathe, Z. Chen, K. Ghosh, H. Kajbaf, S. Frei, M. Sorensen, D. Pommerenke, and J. Min, "Spectrum analyzer-based phase measurement for near-field EMI scanning," *IEEE Trans. Electromagn. Compat.*, vol. 62, no. 3, pp. 848–858, Jun. 2020, doi: 10.1109/TEMC.2019.2920344.
[40] G. Gradoni, D. M. Ramapriya, S. C. Creagh, G. Tanner, M. H. Baharuddin, H. Nasser, C. Smartt, and D. W. P. Thomas, "Near-field scanning and propagation of correlated low-frequency radiated emissions," *IEEE Trans. Electromagn. Compat.*, vol. 60, no. 6, pp. 2045–2048, Dec. 2018, doi: 10.1109/TEMC.2017.2778046.
[41] J. Zhou, Y.-F. Shu, J. Li, N. Xia, Z. Gu, and X.-C. Wei, "A measurement verification for EMI source reconstruction method based on amplitude-only near-field scanning," in *Proc. IEEE Int. Symp. Electromagn. Compat. IEEE Asia–Pacific Symp. Electromagn. Compat. (EMC/APEMC)*, May 2018, p. 125, doi: 10.1109/ISEMC.2018.8394086.
[42] S. M. Wu, S.-W. Guan, C.-D. Li, L.-X. Tsai, C.-T. Kuo, M.-K. Hsieh, and C.-H. Su, "Dielectric constant and loss-tangent extraction using near-field technology and phase delay method," in *Proc. IEEE Int. Symp. Electromagn. Compat. IEEE Asia–Pacific Symp. Electromagn. Compat. (EMC/APEMC)*, May 2018, pp. 683–686, doi: 10.1109/ISEMC.2018.8393868.
[43] H. N. Lin, C. H. Wu, J. F. Huang, W. D. Tseng, J. Y. T. Lin, and M. S. Lin, "Near- and far-field shielding effectiveness analysis of magnetic materials and their effect on wireless power charger," in *Proc. IEEE Int. Symp. Electromagn. Compat. IEEE Asia–Pacific Symp. Electromagn. Compat. (EMC/APEMC)*, May 2018, pp. 1071–1076, 2018, doi: 10.1109/ISEMC.2018.8393951.
[44] S. Lange, D. Schroder, C. Hedayat, C. Hangmann, T. Otto, and U. Hilleringmann, "Investigation of the surface equivalence principle on a metal surface for a near-field to far-field transformation by the NFS3000," in *Proc. Int. Symp. Electromagn. Compat. (EMC Europe)*, Sep. 2020, pp. 1–6, doi: 10.1109/EMCEUROPE48519.2020.9245697.
[45] D. Mandaris, R. Vogt-Ardatjew, M. H. Baharuddin, Z. Joskiewicz, M. Szafranska, E. Coca, D. Thomas, and F. Leferink, "Different test site analysis of radiated field measurements of a complex EUT," in *Proc. Int. Symp. Electromagn. Compat. (EMC Europe)*, Sep. 2019, pp. 674–679, doi: 10.1109/EMCEurope.2019.8872051.
[46] M. Messer and M. Kuhn, "Advanced modeling of an isotropic three-axis magnetic field probe using coils and a near field source approach," in *Proc. Int. Symp. Electromagn. Compat. (EMC Europe)*, Sep. 2019, pp. 173–178, doi: 10.1109/EMCEurope.2019.8872100.
[47] Y. Liu, J. Li, C. Hwang, and V. Khilkevich, "Near-field scan of multiple noncorrelated sources using blind source separation," *IEEE Trans. Electromagn. Compat.*, vol. 62, no. 4, pp. 1376–1385, Aug. 2020, doi: 10.1109/TEMC.2020.2991392.

[48] H. Ragazzo, D. Prost, F. Issac, S. Faure, J. Carrey, and J. F. Bobo, "Thermo-fluorescent images of electric and magnetic near-fields of a high impedance surface," in *Proc. Int. Symp. Electromagn. Compat. (EMC EUROPE)*, Sep. 2019, pp. 257–260, doi: 10.1109/EMCEurope.2019.8871884.

[49] M. Xiao, W. Shao, W. Fang, R. Chen, X. Tian, Z. Li, L. Wang, H. Liu, Y. Wang, X. Xu, and Z. He, "Spatial resolution measurement of near-field probe by using two adjacent microstrip lines," in *Proc. 12th Int. Workshop Electromagn. Compat. Integr. Circuits (EMC COMPO)*, Oct. 2019, pp. 189–191, doi: 10.1109/EMCCompo.2019.8919962.

[50] G. Langer, "Near field of an IC," in *Proc. 12th Int. Workshop Electromagn. Compat. Integr. Circuits (EMC Compo)*, 2019, pp. 67–69.

[51] A.-M. Silaghi, R.-A. Aipu, A. De Sabata, and P.-M. Nicolae, "Near-field scan technique for reducing radiated emissions in automotive EMC," in *Proc. IEEE Int. Symp. Electromagn. Compat. IEEE Asia–Pacific Symp. Electromagn. Compat. (EMC/APEMC)*, May 2018, pp. 831–836, doi: 10.1109/ISEMC.2018.8393897.

[52] G. Gradoni, S. C. Creagh, and G. Tanner, "A Wigner function approach for describing the radiation of complex sources," in *Proc. IEEE Int. Symp. Electromagn. Compat. (EMC)*, Aug. 2014, pp. 882–887, doi: 10.1109/ISEMC.2014.6899092.

[53] G. Gradoni, S. C. Creagh, and G. Tanner, "A phase-space approach for propagating field-field correlation functions near stochastic sources," in *Proc. URSI Int. Symp. Electromagn. Theory (EMTS)*, Aug. 2016, pp. 678–681, doi: 10.1109/URSI-EMTS.2016.7571489.

[54] G. Gradoni, L. R. Arnaut, S. C. Creagh, G. Tanner, M. H. Baharuddin, C. Smartt, and D. W. P. Thomas, "Wigner-function-based propagation of stochastic field emissions from planar electromagnetic sources," *IEEE Trans. Electromagn. Compat.*, vol. 60, no. 3, pp. 580–588, Jun. 2018, doi: 10.1109/TEMC.2017.2738329.

[55] M. H. Baharuddin, H. Nasser, C. Smartt, D. W. P. Thomas, G. Gradoni, S. C. Creagh, and G. Tanner, "Measurement and Wigner function analysis of field-field correlation for complex PCBs in near field," in *Proc. Int. Symp. Electromagn. Compat. (EMC Europe)*, Sep. 2016, pp. 7–11, doi: 10.1109/EMCEurope.2016.7739237.

[56] G. P. Nason, H. M. Mader, S. G. Coles, C. B. Connor, and L. J. Connor, "Stationary and non-stationary time series," in *Statistics in Volcanology*. U.K.: Geological Society for IAVCEI, 2006, ch. 11, doi: 10.1144/IAVCEI001.11.

[57] M. Last and R. Shumway, "Detecting abrupt changes in a piecewise locally stationary time series," *J. Multivariate Anal.*, vol. 99, no. 2, pp. 191–214, 2008, doi: 10.1126/scisignal.2001449.Engineering.

[58] S. Adak, "Time-dependent spectral analysis of nonstationary time series," *J. Amer. Stat. Assoc.*, vol. 93, no. 444, pp. 1488–1501, Dec. 1998, doi: 10.2307/2670062.

[59] A. Ramachandra Rao, K. H. Hamed, and H.-L. Chen, "Segmentation of non-stationary time series," in *Nonstationarities in Hydrologic and Environmental Time Series. Water Science and Technology Library*, vol. 45. Dordrecht, The Netherlands: Springer, 2003, pp. 213–252.

[60] M. H. Baharuddin, C. Smartt, M. I. Maricar, D. W. P. Thomas, G. Gradoni, S. C. Creagh, and G. Tanner, "Analysis of nonstationary emissions for efficient characterization of stochastic EM fields," in *Proc. Int. Symp. Electromagn. Compat. (EMC EUROPE)*, Aug. 2018, pp. 208–213, doi: 10.1109/EMCEurope.2018.8485104.

[61] J. Benesty, M. M. Sondhi, Y. Huang, and S. Greenberg, *Springer Handbook of Speech Processing*. Berlin, Germany: Springer, 2009.

[62] M. Jalil, F. A. Butt, and A. Malik, "Short-time energy, magnitude, zero crossing rate and autocorrelation measurement for discriminating voiced and unvoiced segments of speech signals," in *Proc. Int. Conf. Technological Adv. Electr., Electron. Comput. Eng. (TAEECE)*, May 2013, pp. 208–212, doi: 10.1109/TAEECE.2013.6557272.

[63] T. T. Swee, S. H. S. Salleh, and M. R. Jamaludin, "Speech pitch detection using short-time energy," in *Proc. Int. Conf. Comput. Commun. Eng. (ICCCE)*, May 2010, pp. 11–13, doi: 10.1109/ICCCE.2010.5556836.

[64] M. Mijanur and M. Al-Amin, "Continuous Bangla speech segmentation using short-term speech features extraction approaches," *Int. J. Adv. Comput. Sci. Appl.*, vol. 3, no. 11, 2012, doi: 10.14569/ijacsa.2012.031121.

[65] N. Erdöl, C. Castelluccia, and A. Zilouchian, "Recovery of missing speech packets using the short-time energy and zero-crossing measurements," *IEEE Trans. Speech Audio Process.*, vol. 1, no. 3, pp. 295–303, Jul. 1993, doi: 10.1109/89.232613.

[66] S. KumarBanchhor and A. Khan, "Musical instrument recognition using zero crossing rate and short-time energy," *Int. J. Appl. Inf. Syst.*, vol. 1, no. 3, pp. 16–19, Feb. 2012, doi: 10.5120/ijais12-450131.

[67] J. Wang, K. Zhao, F. Wang, Y. Yang, and Y. Guan, "Application of short-time energy method in the analysis of mechanical vibration signal of circuit breaker," in *Proc. IEEE 3rd Int. Elect. Energy Conf. (CIEEC)*, 2019, pp. 121–125.

[68] D. Lai, X. Zhang, K. Ma, Z. Chen, W. Cehn, H. Zhang, H. Yuan, and L. Ding, "Automated detection of high frequency oscillations in intracranial EEG using the combination of short-time energy and convolutional neural networks," *IEEE Access*, vol. 7, pp. 82501–82511, 2019, doi: 10.1109/ACCESS.2019.2923281.

[69] S. Nandini and A. Shenbagavalli, "Voiced/unvoiced detection using short term processing," *Int. J. Comput. Appl.*, vol. 2, pp. 39–43, 2014.

[70] I. A. Darmawan, "Perbandingan metode zcr dan autocorrelation untuk menghitung frekuensi pada gambelan gender wayang," *J. Ilmu Komput.*, vol. 8, no. 2, pp. 1–6, 2015.

[71] L. R. Rabiner and R. W. Schafer, *Digital Processing of Speech Signals*. Englewood Cliffs, NJ, USA: Prentice-Hall, 1978.

[72] S. S. Bharali and S. K. Kalita, "Zero crossing rate and short term energy as a cue for sex detection with reference to assamese vowels," in *Proc. Int. Conf. Converg. Technol.*, Apr. 2014, pp. 1–4, doi: 10.1109/I2CT.2014.7092124.

[73] R. M. Hanifa, K. Isa, S. Mohamad, S. M. Shah, S. S. Nathan, R. Ramle, and M. Berahim, "Voiced and unvoiced separation in Malay speech using zero crossing rate and energy," *Indones. J. Electr. Eng. Comput. Sci.*, vol. 16, no. 2, pp. 775–780, 2019, doi: 10.11591/ijeecs.v16.i2.pp775-780.

[74] D. Ridha and S. Suyanto, "Removing unvoiced segment to improve text independent speaker recognition," in *Proc. 2nd Int. Seminar Res. Inf. Technol. Intell. Syst. (ISRITI)*, Dec. 2019, pp. 50–53, doi: 10.1109/ISRITI48646.2019.9034578.

[75] D. Nath and S. K. Kalita, "An effective age detection method based on short time energy and zero crossing rate," in *Proc. 2nd Int. Conf. Bus. Inf. Manage. (ICBIM)*, Jan. 2014, pp. 99–103, doi: 10.1109/ICBIM.2014.6970942.

[76] A. M. Fiori and M. Zenga, "Karl Pearson and the origin of kurtosis," *Int. Statist. Rev.*, vol. 77, no. 1, pp. 40–50, Apr. 2009, doi: 10.1111/j.1751-5823.2009.00076.x.

[77] B. Biswal, V. Eadara, D. K. Bebarta, and G. Sahu, "Robust segmentation of optic disc and optic cup using statistical kurtosis test," *Int. J. Imag. Syst. Technol.*, vol. 30, no. 3, pp. 527–543, Sep. 2020, doi: 10.1002/ima.22389.

[78] L. T. DeCarlo, "On the meaning and use of kurtosis," *Psychol. Methods*, vol. 2, no. 3, pp. 292–307, 1998, doi: 10.1016/S0021-9673(98)00845-0.

TITO YUWONO was born in Boyolali, Jawa Tengah, Indonesia, in 1976. He received the B.Eng. and M.Sc. degrees in electrical, electronic, and system engineering from Universiti Kebangsaan Malaysia (UKM), Malaysia, in 2000 and 2005, respectively, where he is currently pursuing the Ph.D. degree in elecrical, electronic, and system engineering. He is currently working as a Lecturer with the Department of Electrical, Islamic University of Indonesia.

His current research interests include the study of EM emission of electronic products, computation of electromagnetic, antenna design, and the IoT applications.

MOHD HAFIZ BAHARUDDIN was born in Kelantan, Malaysia, in January 1987. He received the B.Eng. degree in electrical and electronic engineering and the M.Eng. degree in electrical engineering from the Stevens Institute of Technology, Hoboken, NJ, USA, in 2009 and 2011, respectively, and the Ph.D. degree in electrical and electronic engineering with the University of Nottingham, Nottingham, U.K., in 2019.

He is currently working as a Lecturer with the Department of Electrical, Electronic and Systems Engineering, Universiti Kebangsaan Malaysia, Malaysia. His research interests include modeling and experimental methods in electromagnetic compatibility focusing on the characterization of the stochastic electromagnetic fields in the near field and microwave imaging.

NORBAHIAH MISRAN (Senior Member, IEEE) received the B.Eng. degree in electrical, electronic and system engineering from Universiti Kebangsaan Malaysia (UKM), in 1999, and the Ph.D. degree from the Queen's University of Belfast, Northern Ireland, U.K., in 2004. She was a Tutor at the Department of Electrical, Electronicand System Engineering, UKM, in 1999, where she was a Lecturer, in 2004, an Associate Professor, in 2009, and a Professor, since 2012. She is the author and coauthor of more than 400 research articles in microwave device and system and engineering education. Her research interests include microwave device and system particularly in broadband microstrip antennas, reconfigurable antennas, reflectarray antennas, and metamaterials. She is also conducting some research in engineering education field.

MAHAMOD ISMAIL (Senior Member, IEEE) received the B.Sc. degree in electrical and electronics from the University of Strathclyde, U.K., in 1985, the M.Sc. degree in communication engineering and digital electronics from UMIST, Manchester, U.K., in 1987, and the Ph.D. degree from the University of Bradford, U.K. From 1997 to 1998, he was a Team Engineer in building the first Malaysian microsatellite Tiungsat at Surrey Satellite Technology Ltd., U.K. He became a Guest Professor at the University of Duisburg–Essen (formerly known as Gerhard Mercator Universität Duisburg), Germany, in Summer 2002. He is currently a Professor with the Department of Electrical, Electronics, and System Engineering and the Deputy Director of Research and Education with the Center for Information Technology, Universiti Kebangsaan Malaysia. He has published more than 800 technical articles in journal and proceeding at local and international level. His research interests include mobile communication and wireless networking. He was the Chapter Chair of IEEE Communication Society, Malaysia, and the Educational Activities Chairperson of IEEE Malaysia Section, and is currently a Committee Member of the Joint Chapter Communication and Vehicular Technology Society, IEEE Malaysia. He is also actively involved in conference and became the Technical Program Chairman of Technical Committee and Paper Reviewer.

DAVID W. P. THOMAS (Senior Member, IEEE) received the B.Sc. degree in physics from Imperial College, London, U.K., in 1981, the M.Phil. degree in space physics from Sheffield University, Sheffield, U.K., in 1984, and the Ph.D. degree in electrical engineering from Nottingham University, Nottingham, U.K., in 1990.

He is a Professor of electromagnetics applications and the Director of the George Green Institute for Electromagnetics Research, University of Nottingham. His research interests include EMC, electromagnetic simulation, power system transients, and power system protection. He is a member of CIGRE and a Convenor for Joint Working Group C4.31 EMC between communication circuits and power systems. He is also the Chair of the IEEE Electromagnetic Compatibility (EMC) Technical Committee T7 on Low Frequency EMC, the Chair of COST Action IC 1407 Advanced Characterization and Classification of Radiated Emissions in Densely Integrated Technologies, and a member of the EMC Europe International Steering Committee.

CHRISTOPHER SMARTT received the M.Eng. and Ph.D. degrees in electrical and electronic engineering from the University of Nottingham, Nottingham, U.K., in 1991 and 1995, respectively.

He was a Research Assistant at the University of Nottingham on simulation of microwave devices. He joined BAE SYS-TEMS, where he worked on 2-D and 3-D full field time and frequency domain finite element techniques for electromagnetic field simulation in aerospace applications. In 2007, he rejoined as a Research Fellow with the George Green Institute for Electromagnetics Research, University of Nottingham. His research interests include the development and application of computational electromagnetics methods and the development of electromagnetic field measurement techniques, including time domain and near field methods, with applications to EMC and EMI studies.

HRISTO ZHIVOMIROV (Member, IEEE) was born in Varna, Bulgaria, in 1987. He received the B.Sc. and M.Sc. degrees in communication equipment and technologies from the Technical University of Varna, in 2010 and 2012, respectively, and the Ph.D. degree in theory of communication, in 2016. He is currently an Associate Professor with the Department of Theory of Electrical Engineering and Measurements, Technical University of Varna. His research interests include the field of signal processing, electrical and electronics measurements, MATLAB programming, data acquisition, and data visualization. He is a member of the Federation of Scientific and Technical Unions in Bulgaria and the Union of Scientists in Bulgaria.